

Theoretical study of the elastic breakup of weakly bound nuclei at near-barrier energiesD. R. Otomar,¹ P. R. S. Gomes,² J. Lubian,² L. F. Canto,^{2,3} and M. S. Hussein^{4,5,6}¹*Universidade Estadual do Centro-Oeste, Campus de Irati, PR 153 Km 7, Riozinho, CEP 84500-000, Irati, Paraná, Brazil*²*Instituto de Física, Universidade Federal Fluminense, Avenida Litoranea s/n, Gragoatá, Niterói, 24210-340 Rio de Janeiro, Brazil*³*Instituto de Física, Universidade Federal do Rio de Janeiro, C.P. 68528, Rio de Janeiro, Brazil*⁴*Instituto de Estudos Avançados, Universidade de São Paulo C.P. 72012, 05508-970 São Paulo, Brazil*⁵*Instituto de Física, Universidade de São Paulo, C.P. 66318, 05314-970 São Paulo, Brazil*⁶*Departamento de Física, Instituto Tecnológico de Aeronáutica, DCTA, 12.228-900 São José dos Campos, São Paulo, Brazil*

(Received 12 October 2015; revised manuscript received 13 November 2015; published 22 December 2015)

We have performed continuum discretized coupled channel (CDCC) calculations for collisions of ${}^7\text{Li}$ projectiles on ${}^{59}\text{Co}$, ${}^{144}\text{Sm}$, and ${}^{208}\text{Pb}$ targets at near-barrier energies, to assess the importance of the Coulomb and the nuclear couplings in the breakup of ${}^7\text{Li}$, as well as the Coulomb-nuclear interference. We have also investigated scaling laws, expressing the dependence of the cross sections on the charge and the mass of the target. This work is complementary to that previously reported by us on the breakup of ${}^6\text{Li}$. Here we explore the similarities and differences between the results for the two lithium isotopes. The relevance of the Coulomb dipole and quadrupole strengths at low energy for the two-cluster projectile is investigated in detail.

DOI: [10.1103/PhysRevC.92.064609](https://doi.org/10.1103/PhysRevC.92.064609)

PACS number(s): 24.50.+g, 24.10.Eq, 25.60.Gc, 25.70.Mn

I. INTRODUCTION

Reaction mechanisms in collisions of weakly bound nuclei have been intensively investigated in the last years [1–7], both theoretically and experimentally. These mechanisms may be particularly interesting in collisions of halo nuclei, where the breakup process and its influence on other reaction channels, such as fusion, tend to be very strong. However, the processes involved in collisions of stable weakly bound nuclei, such as ${}^6\text{Li}$, ${}^7\text{Li}$, and ${}^9\text{Be}$, are expected to be qualitatively similar. On the other hand, the intensities of stable beams are several orders of magnitude larger than those presently available for radioactive beams. For this reason, collisions of stable weakly bound nuclei have been widely studied. Since performing direct measurements of breakup cross sections is a very hard task, most experiments determine fusion and elastic cross sections. Recent experiments have shown that transfer processes followed by breakup may predominate over direct breakup of stable weakly bound nuclei at sub-barrier energies [8–11].

In a recent paper [12] we reported continuum discretized coupled channel (CDCC) calculations for collisions of ${}^6\text{Li}$ projectiles with ${}^{59}\text{Co}$, ${}^{144}\text{Sm}$, and ${}^{208}\text{Pb}$ targets at near-barrier energies. We have evaluated Coulomb, nuclear, and total breakup angular distributions, as well as the corresponding integrated cross sections. We have observed strong Coulomb-nuclear interference, and found that the nuclear and the Coulomb components of the breakup cross sections follow scaling laws. For the same E/V_B (energy normalized to the Coulomb barrier), the nuclear component of the breakup cross section is proportional to $A_T^{1/3}$, where A_T is the target's mass number. An explanation for this behavior was later given by Hussein *et al.* [13]. On the other hand, the Coulomb breakup component was shown to depend linearly on the target's atomic number, Z_T . In the present paper we complement the previous work by performing the same kind of analysis for ${}^7\text{Li}$ projectiles.

As in our previous work, the choice of the ${}^{59}\text{Co}$, ${}^{144}\text{Sm}$, and ${}^{208}\text{Pb}$ targets was based on the availability of elastic scattering

data at near-barrier energies. In this way, we were able to check the reliability of our CDCC model by applying it to elastic scattering and comparing the theoretical cross sections with the data.

The paper is organized as follows. In Sec. II the cluster model is discussed and the differences between the low-energy responses of ${}^7\text{Li}$, and ${}^6\text{Li}$ are pointed out. In Sec. III some details of our CDCC model space are given. In Sec. IV the results of our calculation are discussed, while Sec. V is devoted to our conclusions.

II. LOW-ENERGY RESPONSES WITHIN THE CLUSTER MODEL

There are two important differences between the ${}^6\text{Li}$ and ${}^7\text{Li}$ lithium isotopes. The first is that the breakup threshold energy, or Q value, of ${}^6\text{Li}$ is about 1 MeV lower than that of ${}^7\text{Li}$. They are respectively 1.47 and 2.47 MeV. The second difference is that ${}^7\text{Li}$ has a non-zero low-energy dipole strength, in contrast to ${}^6\text{Li}$. Their dipole responses are related to their cluster structure (α - t and α - d for ${}^7\text{Li}$ and ${}^6\text{Li}$, respectively). In fact, using the cluster model, the $B(E\lambda)$ distribution in the projectile $a = c + p$, is given by Refs. [14,15]

$$\begin{aligned} \frac{dB(E\lambda)}{dE_x} &= S N_0^2 \left(\frac{2^{\lambda-1}}{\pi^2} \right) (\lambda!)^2 (2\lambda + 1) \left(\frac{\hbar^2}{\mu_{cp}} \right)^\lambda \\ &\times \frac{Q^{1/2} (E_x - Q)^{\lambda+1/2}}{E_x^{2\lambda+2}} \\ &\times \left[\frac{Z_p A_c^\lambda + (-)^\lambda Z_c A_b^\lambda}{A_a^\lambda} \right]^2 e^2. \end{aligned} \quad (1)$$

In obtaining the above formula, a cluster wave function of a Yukawa form is used: $\phi_{a=c+p}(r) = N_0(\sqrt{K/2\pi}) \exp[-Kr]/r$, with $K = \sqrt{2\mu_{cp}Q/\hbar^2}$, and where μ_{cp} is the reduced mass of the $a = c + p$ system,

S is the cluster structure spectroscopic factor, and N_0 is a normalization constant which takes into account the finite range of the $c + p$ potential r_0 , $N_0 = \exp[Kr_0]/\sqrt{1 + Kr_0}$. The $B(E\lambda)$ values are obtained by integrating the above expression over E_x , to get [16]

$$B(E\lambda) = SN_0^2 \left(\frac{2^{\lambda-1}}{\pi^2} \right) (\lambda!)^2 (2\lambda + 1) \left(\frac{\hbar^2}{\mu_{cp}} \right)^\lambda \times \left[\frac{Z_p A_c^\lambda + (-)^\lambda Z_c A_b^\lambda}{A_a^\lambda} \right]^2 e^2 \frac{1}{Q^{\lambda+1}} \times \frac{(-)^{2\lambda+3} \pi}{(2\lambda + 1)! \sin[(2\lambda + 3/2)\pi]} \prod_{k=1}^{2\lambda+1} (\lambda + 3/2 - k). \quad (2)$$

Thus the dipole $B(E1)$ is given by

$$B(E1) = SN_0^2 \frac{3}{16\pi} \frac{\hbar^2}{\mu_{cp}} \left[\frac{Z_p A_c - Z_c A_p}{A_a} \right]^2 e^2 \frac{1}{Q} \quad (3)$$

and the quadruple $B(E2)$ is

$$B(E2) = SN_0^2 \frac{15}{32\pi} \left(\frac{\hbar^2}{\mu_{cp}} \right)^2 \left[\frac{Z_p A_c^2 + Z_c A_p^2}{A_a^2} \right]^2 e^2 \frac{1}{Q^2}. \quad (4)$$

Using Eqs. (3) and (4), and setting $SN_0^2 = 1$, one finds for ${}^7\text{Li}$ $B(E1) \simeq 0.082 \text{ fm}^2 e^2$ and $B(E2) \simeq 7.0 \text{ fm}^4 e^2$. On the other hand, for ${}^6\text{Li}$ we have $B(E1) = 0.0$ and $B(E2) \simeq 53.5 \text{ fm}^4 e^2$. These results imply a larger dipole Coulomb breakup for ${}^7\text{Li}$ and a larger quadrupole Coulomb breakup for ${}^6\text{Li}$. Of course the quadrupole Coulomb breakup cross section is about 10^{-3} that of the dipole, owing to the smaller number of virtual photons in the former. More details can be found in Ref. [15].

III. THE CDCC MODEL

The most suitable approach to deal with the breakup process, which feeds to the population of states in the continuum, is the so called CDCC method [17,18]. In this type of calculations, the continuum wave functions are grouped into bins, or wave packets, that can be treated similarly to the usual bound excited states, since they are described by square-integrable wave functions. In the present work we use the same assumptions and methodology of the CDCC calculations as Refs. [12,19,20]. We assume that ${}^7\text{Li}$ breaks up directly into an α particle and a tritium nucleus, with separation energy $S_\alpha = 2.47 \text{ MeV}$. To describe the breakup of the projectile into two charged fragments, we used the cluster model. We consider that the two clusters are bound in the ground state of the projectile and that the first bound excited state has spin $1/2^-$ and excitation energy 0.477 MeV . The remaining projectile states are all in the discretized continuum. In all calculations of the present work, we have employed the code FRESKO [21].

In the standard CDCC method [17,18], the scattering of a projectile, composed of a core c (the alpha particle in the present work) and a valence particle p (the triton), by a target

T is modeled by the Hamiltonian

$$H = K_{\text{rel}}(\mathbf{R}) + K_{\text{int}}(\mathbf{r}) + V_{pc} + U_{pT} + U_{cT}, \quad (5)$$

where K_{rel} is the projectile-target relative kinetic motion, K_{int} is projectile internal kinetic energy, V_{pc} is the p - c binding potential, and U_{pT} and U_{cT} are the p - T and c - T optical potentials, respectively. These optical potentials are chosen by the condition of describing the elastic scattering of each cluster from the target. They have an imaginary part arising both from fusion of the cluster with the target and from the excitation of excited states in the target. Thus, the breakup cross sections obtained in standard CDCC calculations correspond only to elastic breakup. However, the influence of inelastic breakup on elastic scattering is taken into account through the action of the imaginary parts of U_{pT} and U_{cT} at the surface region. To go beyond the standard CDCC method, treating target excitations explicitly, one should include in Eq. (5) an additional term corresponding to the internal Hamiltonian of the target. Strictly speaking, in addition to this term, one needs to generalize the fragment-target interactions, in order to include a dependence on the target degrees of freedom [22]. This procedure, however, is not used in the present work, where only excited states of the projectile are included in our channel space.

The sum of the cluster-target potentials of Eq. (5) gives the total interaction between the projectile and the target. It can be written as

$$U(\mathbf{R}, \mathbf{r}) = U_{cT}(\mathbf{R}, \mathbf{r}) + U_{pT}(\mathbf{R}, \mathbf{r}), \quad (6)$$

where \mathbf{R} is the vector joining the centers of mass of the projectile and the target, and \mathbf{r} is the relative position vector between the two clusters. $U(\mathbf{R}, \mathbf{r})$ gives the bare potentials (diagonal matrix elements), and also all couplings among the channels (off-diagonal matrix elements in channel space). This potential contains contributions from Coulomb and from nuclear forces, and the importance of each contribution can be assessed by switching off the other.

The discretization of the continuum is as follows: continuum partial waves up to $l_{\text{max}} = 4$ waves for a density of the continuum discretization of 2 bins/MeV ($l = 0, 1, 2$); 7.7 bins/MeV and 1.92 bins/MeV below and above the $7/2^-$ resonance, respectively; 10 bins/MeV inside the resonance; 2.5 bins/MeV and 2 bins/MeV below and above the $5/2^-$ resonance, respectively; 2.5 bins/MeV inside the resonance; 2 bins/MeV for both $7/2^+$ and $9/2^+$ resonances. The projectile fragments-target potential multipoles up to the term $K_{\text{max}} = 4$ were considered. For the interaction α -tritium to generate the bins, we use an appropriate Woods-Saxon potential to describe the unbound resonant and nonresonant states [19,20]. For the resonant states, we included a spin-orbit interaction. To get a finite set of coupled equations, one must truncate the discretized continuum at some maximal value of the excitation energy and of the orbital angular momentum of clusters. For this reason, rigorous convergence tests have to be performed.

IV. NUMERICAL CALCULATIONS

We have performed CDCC calculations for the ${}^7\text{Li} + {}^{59}\text{Co}$, ${}^7\text{Li} + {}^{144}\text{Sm}$, and ${}^7\text{Li} + {}^{208}\text{Pb}$ systems, for which elastic scattering data at near-barrier energies are available

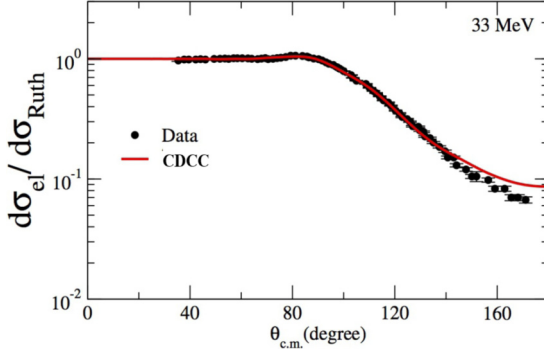


FIG. 1. (Color online) Comparison of elastic scattering data with predictions from our CDCC calculations for ${}^7\text{Li} + {}^{208}\text{Pb}$ at 33.0 MeV. Data are from Ref. [25].

(Refs. [23–25], respectively). To take into account the resonances of ${}^7\text{Li}$, the discretization of the continuum is performed with bins of variable energy width. We use a very fine mesh in the resonance region, where the continuum wave function changes rapidly with the energy, and a mesh with wider spacing away from the resonance.

For the alpha-target and tritium-target optical potentials of Eq. (6), we used the double-folding São Paulo potential [26,27]. The target densities, used in the folding integrals, were taken from the systematics of the São Paulo potential [27]. Assuming that charge and matter densities have similar distributions, the matter density distribution of the triton was obtained by multiplying by 3 the charge distribution reported in Ref. [28]. The matter density of the ${}^4\text{He}$ cluster was obtained through the same procedure. We assumed that the imaginary parts of the optical potentials have the same radial dependence of the real part, with a weaker strength. Then, we adopted the expression, $U_{jT}(r) = [1 + 0.78i]V_{\text{SPP}}(r)$, with j standing for either the alpha or the tritium cluster, and $V_{\text{SPP}}(r)$ standing for the São Paulo potential. This procedure has been able to describe the reaction cross section (and consequently the elastic angular distribution) for many systems in a wide energy interval [29]. Before calculating breakup cross sections, we made sure that our CDCC calculations were able to reproduce elastic scattering data. This is illustrated in Fig. 1, which shows the theoretical and experimental elastic scattering cross sections for ${}^7\text{Li} - {}^{208}\text{Pb}$ scattering at the bombarding energy $E_{\text{lab}} = 33$ MeV. The agreement is good, except for some small discrepancies at backward angles. This is quite satisfactory, if one considers that there is no adjustable parameter in our calculations.

V. DECOMPOSITION OF THE BREAKUP CROSS SECTION INTO NUCLEAR, COULOMB, AND INTERFERENCE PARTS

To study the relative importance of the Coulomb and the nuclear couplings in the breakup process, we adopt the following procedures. First, we separate the diagonal and the off-diagonal parts of the full projectile-target interaction in channel space. Using the spectral representation, it takes the

form

$$U(R, \mathbf{r}) = U_{\text{opt}}(\mathbf{R}, \mathbf{r}) + \Delta U(\mathbf{R}, \mathbf{r}), \quad (7)$$

where the diagonal and the off-diagonal components are respectively

$$U_{\text{opt}} = \sum_i |\phi_i\rangle\langle\phi_i| U |\phi_i\rangle\langle\phi_i| \quad (8)$$

and

$$\Delta U = \sum_{i \neq j} |\phi_i\rangle\langle\phi_i| U |\phi_j\rangle\langle\phi_j|. \quad (9)$$

Above, ϕ_i and ϕ_j represent both the bound eigenfunctions of the projectile and its unbound eigenfunctions, within the continuum discretized approximation. Note that U_{opt} plays the role of an optical potential whereas ΔU is the channel coupling interaction. Further, we split the coupling potential into its Coulomb and nuclear components,

$$\Delta U = \Delta U^{(C)} + \Delta U^{(N)}. \quad (10)$$

Next, we perform three CDCC calculations. In the first we take into account the full interaction $U_{\text{opt}} + \Delta U^{(C)} + \Delta U^{(N)}$. The result is the total breakup cross section, σ_{bup} . In the following, we take into account the potential $U_{\text{opt}} + \Delta U^{(C)}$ (setting $\Delta U^{(N)} = 0$). In this way, we get the Coulomb breakup cross section, $\sigma_{\text{bup}}^{(C)}$. Finally, we run a CDCC calculation for the potential $U_{\text{opt}} + \Delta U^{(N)}$ (setting $\Delta U^{(C)} = 0$), to obtain the nuclear breakup cross section, $\sigma_{\text{bup}}^{(N)}$.

This approach has the disadvantage that the Coulomb-nuclear interference cannot be evaluated directly. It has to be defined as the difference

$$\Sigma_{\text{int}} = \sigma_{\text{bup}} - (\sigma_{\text{bup}}^{(C)} + \sigma_{\text{bup}}^{(N)}). \quad (11)$$

TABLE I. Integrated breakup cross sections for ${}^7\text{Li}$ on ${}^{59}\text{Co}$, ${}^{144}\text{Sm}$, and ${}^{208}\text{Pb}$ targets at energies close to the Coulomb barriers. The first column corresponds to the Coulomb component of the breakup, the next ones to the nuclear component and the total breakup. The last column should be equal to unity if there were no interference between the Coulomb and nuclear components. See text for details.

E/V_B	σ_C (mb)	σ_N (mb)	σ_{bup} (mb)	$(\sigma_{\text{bup}} - \sigma_N)/\sigma_C$
${}^7\text{Li} + {}^{208}\text{Pb}$				
0.84	7.28	0.90	4.51	0.50
1.00	11.20	2.65	10.31	0.68
1.07	16.00	9.18	14.94	0.36
1.30	31.64	11.88	30.48	0.59
${}^7\text{Li} + {}^{144}\text{Sm}$				
0.84	2.49	0.51	0.88	0.15
1.00	6.21	2.50	5.21	0.44
1.07	6.20	6.57	5.11	-0.24
1.30	16.09	8.78	18.71	0.62
${}^7\text{Li} + {}^{59}\text{Co}$				
0.84	0.17	0.05	0.23	1.06
1.00	1.12	1.00	2.10	0.98
1.07	1.84	2.09	3.43	0.73
1.30	4.34	7.08	12.04	1.14

The same approximate procedure as above was employed in Ref. [30] to discuss elastic breakup of halo nuclei at higher energies.

We believe that this approximate method of generating the Coulomb and the nuclear breakup components of the coupled channels-calculated cross section is reasonable for very light targets, such as ^{12}C where the nuclear breakup dominates, and

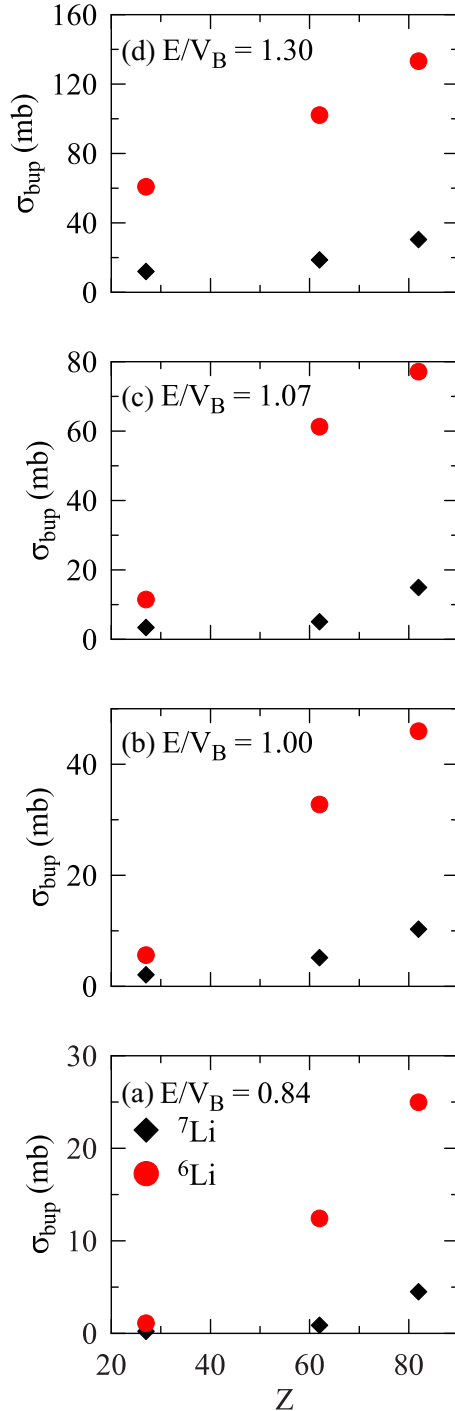


FIG. 2. (Color online) Total breakup cross sections for ^6Li and ^7Li projectiles on ^{59}Co , ^{144}Sm , and ^{208}Pb targets, for energies close to the Coulomb barrier. Results for ^6Li were already published in Ref. [12].

for very heavy targets, such as ^{208}Pb where Coulomb breakup by far dominates. However, we have no way to know how accurate the switching-off method is in the case of medium-mass targets, where both the Coulomb and nuclear components are equally important.

Table I shows the integrated ^7Li breakup cross sections for the three systems at near-barrier energies. As expected, one observes that the Coulomb and the nuclear components, as well as the total breakup cross sections, for the light targets are much smaller than the corresponding cross sections for the heavier targets. The interference between the nuclear and Coulomb breakup amplitudes can be easily observed in the last column of Table I. In the no-interference limit, the quantity $(\sigma_{\text{bup}} - \sigma_N)/\sigma_C$ should be equal to 1. The numbers shown in the table are very different from this limit, which indicates that there is strong Coulomb-nuclear interference in the breakup of ^7Li . The same conclusion was reached in the case of the ^6Li isotope [12].

In Fig. 2 we show the integrated cross sections for the breakup of $^{6,7}\text{Li}$ on ^{59}Co , ^{144}Sm , and ^{208}Pb targets, at three near-barrier energies. The cross sections for ^7Li are results of the present calculations whereas those for ^6Li were taken from Ref. [12]. One observes that, for a given projectile and at the same value of E/V_B , the breakup cross sections increase with the target charge. One sees also that, for each target and at the same relative energy, the cross sections for ^6Li are much larger

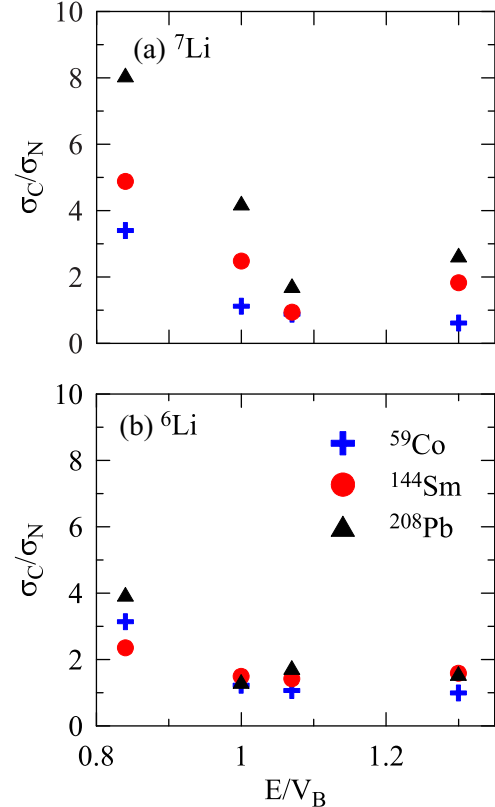


FIG. 3. (Color online) Ratio between Coulomb and nuclear breakup as a function of energy for the ^6Li and ^7Li projectiles on the ^{59}Co , ^{144}Sm , and ^{208}Pb targets.

than those for ${}^7\text{Li}$. This is not surprising, since the breakup threshold energy for ${}^6\text{Li}$ is appreciably smaller than that for ${}^7\text{Li}$.

Using the values of the breakup cross sections given in Table I and the results of Ref. [12], we can plot the ratio σ_C/σ_N as a function of the relative energy. The results for the targets considered in our study are shown in Fig. 3, for the breakup

of ${}^7\text{Li}$ [panel (a)] and for the breakup of ${}^6\text{Li}$ [panel (b)]. One observes that this ratio decreases as E/V_B increases, and that it is systematically larger than 1, except for the breakup of ${}^7\text{Li}$ on the lightest target at above-barrier energies ($E/V_B > 1$). One notices also that, for a given projectile and at a fixed value of E/V_B , the ratio increases with the charge of the target. This

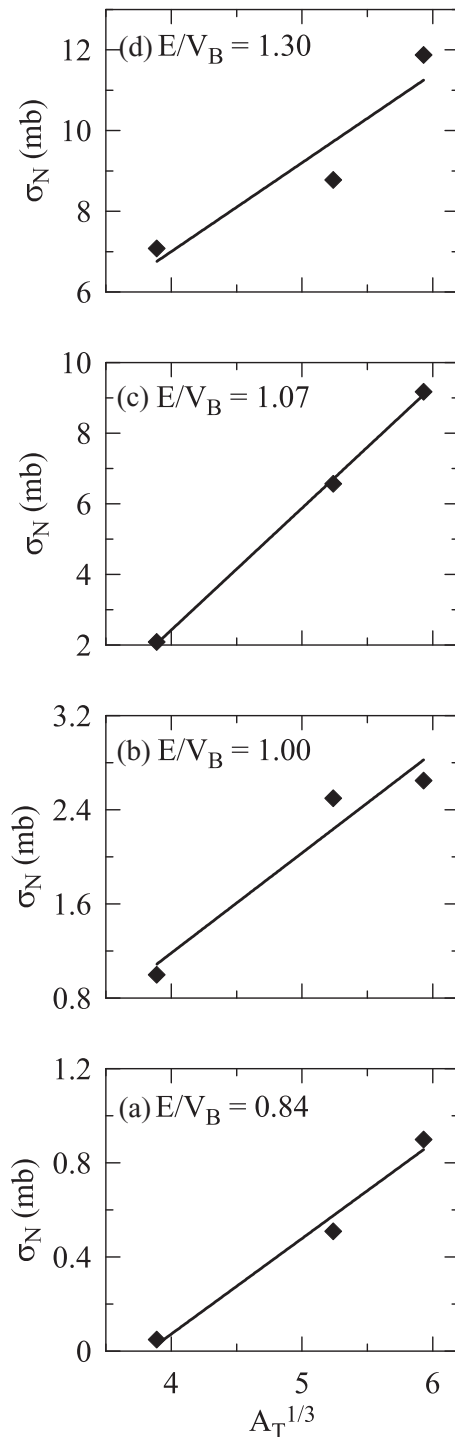


FIG. 4. ${}^7\text{Li}$ nuclear breakup cross sections as a function of the target mass, for ${}^{59}\text{Co}$, ${}^{144}\text{Sm}$, and ${}^{208}\text{Pb}$ targets.

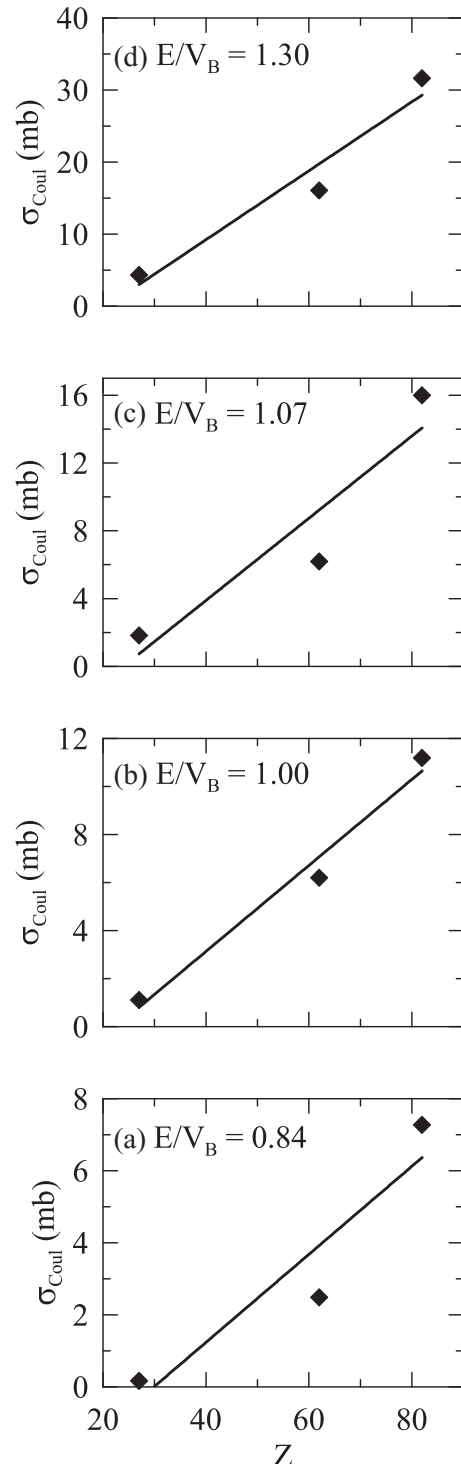


FIG. 5. ${}^7\text{Li}$ Coulomb breakup cross sections as a function of the target charge, for ${}^{59}\text{Co}$, ${}^{144}\text{Sm}$, and ${}^{208}\text{Pb}$ targets.

behavior is expected and it has already been observed for ${}^6\text{Li}$ projectiles [12]. However, the most interesting (and new) result in Fig. 3 is that this ratio for a given target and a given E/V_B is much larger in the breakup of ${}^7\text{Li}$ than in that of ${}^6\text{Li}$. This result should arise from the fact that the low-energy Coulomb dipole response in the breakup of ${}^7\text{Li}$ is larger than in the breakup of ${}^6\text{Li}$. The reason is that the factor $[Z_p A_c - Z_c A_p]^2$, appearing in Eqs. (1) and (3), is equal to 4 for ${}^7\text{Li}$, whereas in the case of ${}^6\text{Li}$ it vanishes identically.

A detailed study of Figs. 2 and 3 leads to a very interesting conclusion. The analysis of Fig. 2 indicated that the breakup cross sections for ${}^6\text{Li}$ are larger than those for ${}^7\text{Li}$, even for the ${}^{208}\text{Pb}$ target. In this case, the Coulomb breakup dominates, as can be seen in Table I (for ${}^7\text{Li}$) and in Ref. [12] (for ${}^6\text{Li}$). However, Coulomb breakup depends on two factors. The first is the low-energy Coulomb dipole response, which vanishes for ${}^6\text{Li}$ and does not for ${}^7\text{Li}$. The second is the low breakup threshold, which is 1 MeV lower in the case of ${}^6\text{Li}$. Figure 2 indicates that the predominant factor is the lower breakup threshold of the ${}^6\text{Li}$ projectile. On the other hand, Fig. 3 indicates that the ratios σ_C/σ_N are systematically larger for the ${}^7\text{Li}$ projectile. The consistency of the two above conclusions would require that the nuclear breakup of ${}^6\text{Li}$ be much larger than that of ${}^7\text{Li}$. This can be checked by comparing σ_N for the two projectiles on the same target and at the same value of E/V_B . Looking at the nuclear breakup cross sections in Table I (for ${}^7\text{Li}$) and at those given in Ref. [12] (for ${}^6\text{Li}$), one concludes that this condition is satisfied. For example, for the ${}^{208}\text{Pb}$ target at $E/V_B = 0.84$, the cross sections for the nuclear breakup of ${}^6\text{Li}$ and for that of ${}^7\text{Li}$ are respectively 8.8 mb and 0.9 mb.

We have also investigated scaling laws in the nuclear and Coulomb components of ${}^7\text{Li}$ breakup. For this purpose, we followed the procedures of Ref. [12] in their study of ${}^6\text{Li}$ breakup. Figure 4 shows plots of σ_N versus $A_T^{1/3}$. One observes that the nuclear components of the breakup cross section at a fixed value of E/V_B increase linearly with $A_T^{1/3}$, to a good

approximation. On the other hand, Fig. 5 shows plots of σ_C versus Z_T . One notices that the cross sections increase with Z_T , showing a roughly linear behavior. These findings are analogous to those of Ref. [12], for the ${}^6\text{Li}$ Lithium isotope.

VI. SUMMARY

In summary, we have extended our investigation of the elastic breakup of weakly bound nuclei to a two-cluster projectile with significant dipole strength at low excitation energy. The current work complements a previous study where no or very weak dipole strength was found. The isotopes of lithium, ${}^7\text{Li}$, studied in the current paper, and ${}^6\text{Li}$ are used for the purpose of comparison. We have found the same qualitative behavior in both cases, involving the Coulomb, nuclear, and interference parts of the breakup cross section; namely, a strong interference term and similar scaling laws for both the Coulomb and nuclear components of the breakup cross section, i.e., increasing linearly with $A_T^{1/3}$ and Z_T , respectively, for the same relative energy. The comparison of ${}^7\text{Li}$ with the ${}^6\text{Li}$ elastic breakup shows that the ${}^6\text{Li}$ total breakup and its nuclear and Coulomb components are greater than those for ${}^7\text{Li}$, for the same targets and relative energies, whereas the ratios of Coulomb to nuclear components are much larger for ${}^7\text{Li}$ than for the corresponding ones of the ${}^6\text{Li}$ system. We interpret those results in terms of the smaller breakup Q value in ${}^6\text{Li}$ and the low-energy Coulomb dipole strengths of the lithium isotopes. The results also indicate the importance of the Coulomb breakup through the excitation of higher multipolarities (quadrupole, octopole, etc.) in the $\alpha + d$ cluster component of the ${}^6\text{Li}$ wave function.

ACKNOWLEDGMENTS

We thank Pierre Descouvemont for useful comments. The authors acknowledge financial support from CNPq, CAPES, FAPERJ, and FAPESP.

-
- [1] L. F. Canto, P. R. S. Gomes, R. Donangelo, and M. S. Hussein, *Phys. Rep.* **424**, 1 (2006).
- [2] J. F. Liang and C. Signorini, *Int. J. Mod. Phys. E* **14**, 1121 (2005).
- [3] N. Keeley, R. Raabe, N. Alamanos, and J. L. Sida, *Prog. Part. Nucl. Phys.* **59**, 579 (2007).
- [4] N. Keeley, N. Alamanos, K. W. Kemper, and K. Rusek, *Prog. Part. Nucl. Phys.* **63**, 396 (2009).
- [5] K. Hagino and N. Takigawa, *Prog. Theor. Phys.* **128**, 1061 (2012).
- [6] B. B. Back, H. Esbensen, C. L. Jiang, and K. E. Rehm, *Rev. Mod. Phys.* **86**, 317 (2014).
- [7] L. F. Canto, P. R. S. Gomes, R. Donangelo, J. Lubian, and M. S. Hussein, *Phys. Rep.* **596**, 1 (2015).
- [8] D. H. Luong *et al.*, *Phys. Lett. B* **695**, 105 (2011).
- [9] D. H. Luong, M. Dasgupta, D. J. Hinde, R. du Rietz, R. Rafiei, C. J. Lin, M. Evers, and A. Diaz-Torres, *Phys. Rev. C* **88**, 034609 (2013).
- [10] R. Rafiei, R. du Rietz, D. H. Luong, D. J. Hinde, M. Dasgupta, M. Evers, and A. Diaz-Torres, *Phys. Rev. C* **81**, 024601 (2010).
- [11] A. Shrivastava *et al.*, *Phys. Lett. B* **633**, 463 (2006).
- [12] D. R. Otomar, P. R. S. Gomes, J. Lubian, L. F. Canto, and M. S. Hussein, *Phys. Rev. C* **87**, 014615 (2013).
- [13] M. S. Hussein, P. R. S. Gomes, J. Lubian, D. R. Otomar, and L. F. Canto, *Phys. Rev. C* **88**, 047601 (2013).
- [14] C. A. Bertulani and M. S. Hussein, *Nucl. Phys. A* **526**, 751 (1991).
- [15] C. A. Bertulani, M. S. Hussein, and G. Münzenberg, *Physics of Radioactive Beams* (Nova Science, New York, 2001).
- [16] M. S. Hussein and R. Lichtenthäler, *Phys. Rev. C* **77**, 054609 (2008).
- [17] M. Kamimura, M. Yahiro, Y. Iseri, Y. Sakuragi, H. Kameyama, and M. Kawai, *Prog. Theor. Phys. Suppl.* **89**, 1 (1986).
- [18] N. Austern, Y. Iseri, M. Kamimura, M. Kawai, G. Rawitscher, and M. Yahiro, *Phys. Rep.* **154**, 125 (1987).
- [19] D. R. Otomar, J. Lubian, P. R. S. Gomes, D. S. Monteiro, O. A. Capurro, A. Arazi, J. O. Fernández Niello, J. M. Figueira, G. V. Martí, D. Martínez Heimann, A. E. Negri, A. J. Pacheco, V. Guimarães, and L. C. Chamon, *Phys. Rev. C* **80**, 034614 (2009).

- [20] D. R. Otomar, J. Lubian, and P. R. S. Gomes, *Eur. Phys. J. A* **46**, 285 (2010).
- [21] I. J. Thompson, *Comput. Phys. Rep.* **7**, 167 (1988).
- [22] M. Yahiro, Y. Iseri, H. Kameyama, M. Kamimura, and M. Kawai, *Prog. Theor. Phys. Suppl.* **89**, 32 (1986).
- [23] F. A. Souza, L. A. S. Leal, N. Carlin, M. G. Munhoz, R. Liguori Neto, M. M. de Moura, A. A. P. Suaide, E. M. Szanto, A. Szanto de Toledo, and J. Takahashi, *Phys. Rev. C* **75**, 044601 (2007).
- [24] J. M. Figueira, J. O. Fernández Niello, A. Arazi, O. A. Capurro, P. Carnelli, L. Fimiani, G. V. Martí, D. Martinez Heimann, A. E. Negri, A. J. Pacheco, J. Lubian, D. S. Monteiro, and P. R. S. Gomes, *Phys. Rev. C* **81**, 024613 (2010).
- [25] N. Keeley *et al.*, *Nucl. Phys. A* **571**, 326 (1994).
- [26] L. C. Chamon, D. Pereira, M. S. Hussein, M. A. Cândido Ribeiro, and D. Galetti, *Phys. Rev. Lett.* **79**, 5218 (1997).
- [27] L. C. Chamon, B. V. Carlson, L. R. Gasques, D. Pereira, C. De Conti, M. A. G. Alvarez, M. S. Hussein, M. A. Cândido Ribeiro, E. S. Rossi, Jr., and C. P. Silva, *Phys. Rev. C* **66**, 014610 (2002).
- [28] D. Abbott *et al.*, *Eur. Phys. J. A* **7**, 421 (2000).
- [29] L. R. Gasques, L. C. Chamon, P. R. S. Gomes, and J. Lubian, *Nucl. Phys. A* **764**, 135 (2006).
- [30] M. S. Hussein, R. Lichtenthaler, F. M. Nunes, and I. J. Thompson, *Phys. Lett. B* **640**, 91 (2006).